TWO DIMENSIONAL FLUID THEORY OF FIELD-ALIGNED IRREGULARITIES IN METEOR TRAILS

Meers M. Oppenheim and Lars P. Dyrud

Center for Space Physics, Boston U., 725 Comm. Ave., Boston, MA 02215 U.S.A., Email meerso@bu.edu

ABSTRACT

Meteor trails created by the ablation of micro-meteoroids between 70 and 130 km altitude in the atmosphere create columns of plasma often with densities that exceed the ambient ionospheric plasma density by orders of magnitude. Density gradients at the edges of these trails can create ambipolar electric fields with amplitudes in excess of hundreds of mV/m. These fields, in turn, drive Farley-Buneman and gradient-drift (FBGD) instabilities which create field-aligned plasma density irregularities detectable by large aperture radars. This paper presents a new theory of meteor trail instabilities and compares this theory with simulations, observations, and related theories.

INTRODUCTION AND BACKGROUND

Radars probing the atmosphere between 70 km and 130 km frequently receive echoes from plasma trails left by passing and disintegrating meteors. These echoes have proven useful in characterizing small meteors and in estimating atmospheric temperatures and wind velocities. Two distinct types of radar echoes return from meteor trails. Strong echoes return when the radar pointing direction lies perpendicular to the meteoroid's trajectory, creating a "specular" reflection [4]. Weaker echoes are frequently observed by highly sensitive, large-aperture, radars not pointing perpendicular to the trail's orientation, creating echoes labeled as "non-specular" reflections [6, 21]. Non-specular have been attributed to the Farley–Buneman/gradient–drift (FBGD) instability mechanism [6, 5]. In an earlier paper, we used simulations to show that non-specular echoes can easily result from the FBGD instability which rapidly develops into plasma turbulence [17]. In a subsequent paper we showed that FBGD waves develop without an external electric field and also demonstrated that the waves and turbulence cause an anomalous diffusion much larger than the expected cross-field ambipolar diffusion [9]. This paper develops the linear plasma fluid instability theory of these trails and predicts the altitude range at which one expects to find field–aligned irregularities (FAI) and therefore non–specular meteor trails.

The fundamental behavior of meteor trails and collisionally dominated plasmas has been discussed in many books and review articles [16, 3, 19]. More specifically, a number of authors have evaluated the ambipolar diffusion of meteor trails in collisional plasmas [18, 13]. Most of our understanding of weakly ionized meteor trails derives from radar observations and relies on detailed analyses of the precise interaction between meteor trails and radar signals [12].

THEORY OF METEOR TRAIL PLASMA

A small meteoroid ($<\sim 10^{-5}$ kg) ablating in the upper atmosphere creates a narrow column of energetic neutrals and plasma. This column expands rapidly until slowed, partially ionized, and cooled by collisions. The radius of the column at the point when it transitions from a rapid kinetic expansion to a slower diffusive expansion is called the initial radius of the trail and it appears to be somewhat smaller than the mean free path length [1, 2]. After the column reaches this initial radius, the dynamics of the expanding column of charged particles may be approximately described as a plasma fluid.

Above 75km in altitude and perpendicular to the geomagnetic field, $\mathbf{B}$, electrons are highly magnetized while ions are de-magnetized by collisions. Hence, as the trail plasma expands beyond its initial radius, a strong ambipolar electric field develops as a result of the differing ion and electron mobilities. The electrons respond to this cross-field ambipolar field by $\mathbf{E}\times\mathbf{B}$–drifting perpendicular to both $\mathbf{B}$ and the density gradient of the meteor trail. This drift, combined with a diamagnetic drift caused by the plasma density gradients, can generate an unstable plasma [10]. This instability leads to the formation of waves which rapidly develop into turbulence. This field aligned instability also creates plasma density perturbations visible to radars, allowing for non-specular radar reflections. Further it causes anomalous diffusion, effecting the meteor trail's expansion rate. The following sections describe how the electric fields, electron drifts, and instabilities depend upon the altitude and trail density.

EQUILIBRIUM CONDITION

In order to evaluate the stability of a meteor trail, we must first define an equilibrium state. We will use the ambipolar expansion of a diffusing plasma column perpendicular to the magnetic field. We conduct this analysis only in the plane perpendicular to $\mathbf{B}$ and assume that in the plane parallel to $\mathbf{B}$ the trail expands through ambipolar diffusion and is not unstable to plasma instabilities [14]. To define the equilibrium state we will assume the ions are an inertialess, isothermal, collisional, and unmagnetized fluid plasma where

$$\mathbf{v}_i = -\mu_i \nabla\phi - D_i \nabla s \tag{1}$$

and $\mu_{i,e} \equiv e/(m_{i,e}\nu_{i,e})$ defines the ion and electron mobilities, $D_{i,e} \equiv kT_{i,e}/(m_{i,e}\nu_{i,e})$ defines the ion and electron diffusion rates, ϕ is the electric potential, and $\nabla s \equiv \nabla n/n = \nabla \ln(n/n_b)$ defines the gradient of the log of the plasma density normalized to the background density, n_b. The electrons are an inertialess and magnetized fluid whose velocity perpendicular to $\mathbf{B}$ can be expressed as

$$\mathbf{v}_{e\perp} = \mu_{e\perp}\nabla\phi - D_{e\perp}\nabla s \quad + \quad \frac{\mathbf{v}_{E\times B} + \mathbf{v}_D}{1+\nu_e^2/\Omega_e^2}, \qquad (2)$$

$$\mu_{e\perp} \equiv \frac{\mu_e}{1+\Omega_e^2/\nu_e^2} \quad , \quad D_{e\perp} \equiv \frac{D_e}{1+\Omega_e^2/\nu_e^2},$$

$$\mathbf{v}_{E\times B} \equiv \frac{\mathbf{E}\times\mathbf{B}}{B^2} \quad , \quad \mathbf{v}_D \equiv -\frac{kT_e}{e}\frac{\nabla s\times\mathbf{B}}{B^2},$$

$\mathbf{v}_D$ is the diamagnetic drift, and $\Omega_e = eB/m_e$ is the electron cyclotron frequency (see [7], p. 171, for an explanation of these terms). For altitudes above 85 km, $\Omega_e^2/\nu_e^2 \gg 1$ and electrons predominantly engage in $\mathbf{E}\times\mathbf{B}$ and diamagnetic drifts, as described by third term of eqn. (3).

The assumption of quasi-neutrality, $\nabla\cdot\mathbf{J} = 0$, allows us to generate an expression for the potential ($\perp$ to $\mathbf{B}$) in terms of density,

$$\mu_T\nabla\cdot(n\nabla\phi) - D_T\nabla^2 n + \frac{\nabla n\cdot\nabla\phi\times\mathbf{B}_0}{1+\Omega_e^2/\nu_e^2} = 0 \qquad (3)$$

where $D_T \equiv D_{e\perp} - D_i$ and $\mu_T \equiv \mu_{e\perp} + \mu_i$. This equation allows us to solve for the cross-field ambipolar electric potential, ϕ, for a prescribed density distribution, n, and vise-versa.

In many configurations eqn. 3 becomes easy to evaluate. One simple trail geometry in Cartesian coordinates aligns the magnetic field, $\mathbf{B}$, along the $\hat{y}$ direction; allows the density gradient to vary only along $\hat{x}$; and assumes homogeneity along both $\hat{y}$ and $\hat{z}$. While homogeneity along $\mathbf{B}$ is unrealistic, at high altitudes one expects trails stretched in the direction parallel to $\mathbf{B}$, so this assumption is not entirely unrealistic. An alternate geometry which may be evaluated in cylindrical coordinates aligns the trail parallel to $\mathbf{B}$, leaving a circular cross-section perpendicular to $\mathbf{B}$. As long as ∇n is perpendicular to $\mathbf{E}\times\mathbf{B}$, eqn. (3) becomes simply, $\nabla\cdot(n\nabla\phi) = D_T/\mu_T\nabla^2 n$, and may be easily solved for either slab or cylindrical geometries.

In the case of a slab trail, $E_x = -\frac{D_T}{\mu_T}\frac{\partial s}{\partial x} + \frac{C}{n}$, where C is a constant of integration set by boundary conditions. If we further assume that the density of the trail is the sum of a Maxwellian plus a background density, $n = n_0\exp(-x^2/x_0^2) + n_b$, then the ambipolar field becomes

$$E_x = -\frac{D_T}{\mu_T}\left[\frac{n_0\exp(-x^2/x_0^2)(-2x/x_0^2)}{n_0\exp(-x^2/x_0^2)+n_b}\right]. \qquad (4)$$

At 105km, the ion cross-field mobility, μ_i exceeds the electron one, $\mu_{e\perp}$. In this case, the electric field points toward the center of the trail and prevents the ions from escaping from the magnetized and less mobile electrons. At different altitudes, the changing collision rates alter the relationship between these mobilities. Below

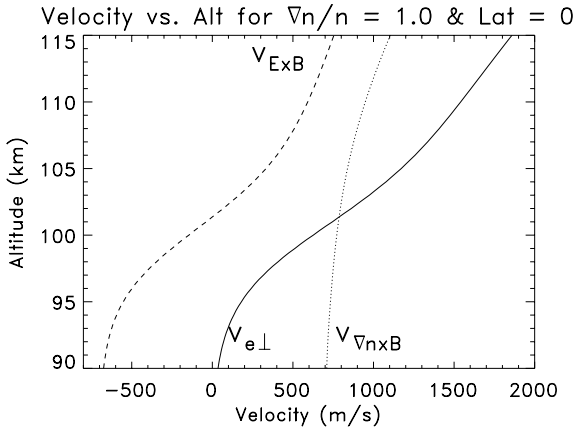

Figure 1. Velocity vs. altitude assuming parameters from the international reference ionosphere (IRI) for the equator. $v_{\mathbf{E}\times\mathbf{B}}$ shows the $\mathbf{E}\times\mathbf{B}$ drift velocity; $v_{\nabla n\times\mathbf{B}}$ shows the diamagnetic drift velocity; and $v_{e\perp}$ shows the sum of the two velocities.

~ 100 km (near the equator), the collision rates become high enough that the electron diffusion rate exceeds the ion rate causing the ambipolar electric field to reverse directions. The transition altitude where $\mathbf{E}$ shifts from inward to outward pointing depends on latitude because of the changing geomagnetic field. This altitude also plays less of a role in the generation of instabilities than one might expect, because the instability driver results from the total electron drift speed, which derives from a combination of $\mathbf{E}\times\mathbf{B}$ and diamagnetic drifts as discussed in the following section.

ELECTRON DRIFT

Electron drift motion results from the combination of $\mathbf{E}\times\mathbf{B}$ and diamagnetic drifts where, in the absence of external electric fields or, equivalently, neutral winds, E arises from the self-generated ambipolar electric fields. Combining eqns. (3) and () makes the electron drift velocity

$$\mathbf{v}_{e\perp} = \left(\frac{D_T}{\mu_T} + \frac{D_e}{\mu_e}\right)\frac{\nabla s\times\hat{B}}{|B|} - \left(\mu_{e\perp}\frac{D_T}{\mu_T} + D_{e\perp}\right)\nabla s \qquad (5)$$

where $\hat{B} \equiv \mathbf{B}/|B|$. In the case where electron motion lies purely perpendicular to ∇n, this simplifies to

$$v_{e\perp} \quad = \quad \frac{C_s^2}{\Omega_i(1+\Psi_0)}\nabla s\times\hat{B} \qquad (6)$$

where $C_s^2 = \sqrt{k(T_e+T_i)/m_i}$ is the ion acoustic velocity and $\Psi_0 \equiv \frac{\nu_e\nu_i}{\Omega_e\Omega_i}$, a ratio that shows up repeatedly in E-region dynamics. This equation tells us that, regardless of the direction of $\mathbf{E}$, the electrons always drift in the positive $\nabla n\times\hat{B}$ direction. At high altitudes $\mathbf{E}\times\mathbf{B}$ drifting dominates, but at lower altitudes, as $\mathbf{E}$ changes sign, the electrons continue to drift in the same direction. This occurs because the diamagnetic drift rate, $\mathbf{v}_D$, becomes larger, preventing the electrons from reversing direction. Figure 1 compares drift velocities as a function of altitude for a trail with $\nabla s = 1\,\mathrm{m}^{-1}$. For larger (or

smaller) values of ∇s, the velocities scale linearly with ∇s. This rapid drift motion drives the instabilities discussed in Dyrud et al. [9] and Oppenheim et al. [17].

STABILITY

Linear plasma theory allows us to evaluate the stability of these meteor trails. Further, it teaches us about the phase and group velocities and growth or damping of any wave which might develop within the trail. Since radars are extremely sensitive to plasma waves, understanding the characteristics of these waves should allow us to better understand non–specular radar echoes.

The simplest linear analysis assumes both the electrons and ions behave as plasma fluids and recreates the dispersion relation described in Fejer et al. [11]. To obtain the dispersion relation, assume inertialess electrons as in eqn. (3) and quasineutrality as before, but keep ion inertia. The linear, Fourier transformed, ion momentum equation remains the same as eqn. (1) except $\nu_i \rightarrow \nu_i - i\omega$ where ω is the complex wave frequency. With these assumptions the following relation may be derived:

$$\omega - \mathbf{k}\cdot\mathbf{v}_{e0} = -A\left[(\omega - \mathbf{k}\cdot\mathbf{v}_{i0})(\nu_i - i\omega) + ik^{\dagger 2}C_s^2\right] \quad (7)$$

$$A \equiv \left(\frac{\Psi_0}{\nu_i} - \frac{i}{\Omega_i}\frac{\mathbf{k}\cdot\nabla s_0 \times \hat{B}}{k^{\dagger 2}}\right) \quad (8)$$

where $\mathbf{v}_{i0}$ and $\mathbf{v}_{e0}$ are the equilibrium (drift) velocities of each species; $\nabla s_0 \equiv \nabla n_0/n_0$ is the initial density gradient scale length; $k^{\dagger 2} \equiv (\mathbf{k} - i\nabla s_0)\cdot\mathbf{k}$.

For the case of meteor trails ω_r often has a similar magnitude as ν_i and, therefore, one must solve eqn. (7) as a quadratic equation. Two assumptions allow some simplification of eqn. (7). If $\mathbf{B} = \mathbf{B}_0\hat{z}$ and $\mathbf{v}_{i0}$ is negligible compared to $\mathbf{v}_{e0}$, then

$$A \equiv \Psi_0/\nu_i - (i/\Omega_i)\mathbf{k}\cdot\nabla s_0 \times \hat{z}/k^{\dagger 2} \text{ and}$$
$$\omega - \mathbf{k}\cdot\mathbf{v}_{e0} = -A[(\nu_i\omega - i\omega^2) + ik^{\dagger 2}C_s^2]\,. \quad (9)$$

One interesting point follows: In FBGD theory, the $\mathbf{k}\cdot\mathbf{v}_{e0}$ term drives the instability. For meteor trails, with no driving external electric field, the $Aik^2C_s^2$ term also contains a real component which always exceeds the $\mathbf{k}\cdot\mathbf{v}_{e0}$ term such that adding the real components of the two terms yields

$$\Re[Aik^2C_s^2 - \mathbf{k}\cdot\mathbf{v}_{e0}] = \frac{C_s^2 k\cdot\nabla s_0\times\hat{B}}{\Omega_i}\frac{\Psi_0}{1+\Psi_0}\,. \quad (10)$$

This assumes that $\nabla s_0 \cdot k/k^2 \ll 1$, which applies when $\mathbf{k}$ represents waves aligned mostly perpendicular to the gradient, ∇s.

Though fig. 2 shows increasing growth rates for increasing values of $|k|$, the simulation shows a peak wavelength at $\sim$ 20 cm. However, the fluid theory ignores kinetic plasma phenomena. In particular, at these short wavelengths, we expect ion Landau damping to reduce the growth rate short wavelength modes [20, 15]. The fluid equations most accurately represent the physics at the longest unstable wavelengths and, in the discussion below, we will limit ourselves to that case.

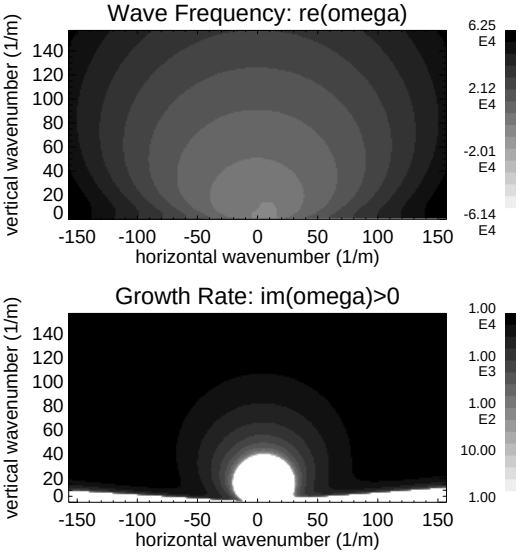

Figure 2. Shows the real (top) and imaginary (bottom) parts of ω as a function of vertical and horizontal wavenumber, $\mathbf{k}$. Of the two roots the one with the larger ω_i is shown and the bottom panel only shows values for $\omega_i > 0$.

CRITERION FOR INSTABILITY ONSET

While eqn. (9) may not be appropriate to predict the growth rate of the instability for all wavelengths, it does provide an approximation for the instability threshold. Figure 3 shows positive growth rates as a function of altitude and peak plasma density for meteor trails having a Maxwellian density profile, $n = n_0\exp(-r^2/r_0^2) + n_b$. To set the crucial scale length, r_0, we used two initial radius measurements: the [2] prediction and the smaller [1] measurement. To limit the very short wavelength modes, we required that the instability develop a positive growth rate for waves longer than twice the Debye length. The results are only weakly sensitive to changes in this criterion. One can see that the instability growth rate depends strongly on the initial radius and only weakly on the peak plasma density. The minimum altitude is mostly determined by the high collision rates and depends only weakly on meteor parameters.

The maximum instability altitude is set principally by the initial radius of the trail which determines ∇s. The Bronshten [2] values allow us to predict instability over a limited altitude range. The smaller radii predicted by Baggaley [1] lead us to predict essentially no ceiling on the instability altitude.

The observational data appears to predict a limited range of altitudes over which trails become unstable. The trail echoes almost invariably span a smaller range of altitudes than do the associated head echoes. This difference occurs frequently and is discussed in more detail in Close et al. [8].

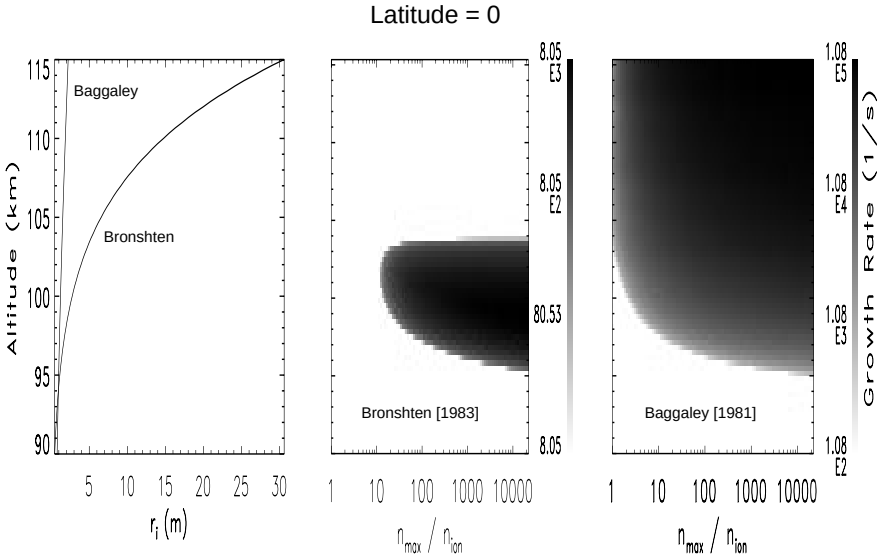

Figure 3. Left panel plots initial radius of trail versus altitude for the Baggaley and Bronshten models. The center panel shows the predicted growth rate as a function of altitude and peak plasma density, n_0/n_b, for the radius suggested by the Bronshten model. The left panel shows the same for the radius suggested by the Baggaley model.

CONCLUSIONS

We have used a fluid description of meteor trail plasma dynamics to better understand the results from both simulations and large-aperture radar observations. We have solved for the equilibrium state of a diffusing meteor trail perpendicular to $\mathbf{B}$ and shown that both the electron diamagnetic drift and $\mathbf{E}\times\mathbf{B}$ drift contribute to the total electron drift. Further, this total electron drift is always in the $\nabla n \times \mathbf{B}$ direction, even when the $\mathbf{E}\times\mathbf{B}$ drift drives electrons in the opposite direction.

We then solved the linear, perturbed system of equations around this equilibrium state, showing that standard FBGD assumptions do not apply to meteor trails and that it is necessary to solve the complete quadratic dispersion relation. Nevertheless, one may use this equation to calculate the range of wavelengths over which instability may occur and the characteristics of the resulting waves.

Making a number of assumptions about the state of "typical" meteor trails, we solved this dispersion relation, showing the limited range of altitudes at which one expects instability growth. The minimum altitude depends principally on the composition and latitude of the trail. The maximum altitude depends primarily on the gradient scale length of the trail which results from the initial radius of the meteor trail. We used this dependency to show that the Bronshten [2] description of initial radius better matches observations, than the description put forth by [1].

Acknowledgments: The authors would like to thank Kelly McMillon and Licia Ray for editing and producing many of the figures. This material is based upon work partially supported by the National Science Foundation under Grant No. ATM9986976 and NASA Grant No. NGT5-50288.

REFERENCES

[1] Baggaley W.J., 1981, Bull. Astron. Inst. Czech., 32, 345

[2] Bronshten V.A., 1983, Physics of Meteoric Phenomena, chap. 100-105, Reidel Publishing Company

[3] Ceplecha Z., Borovicka J., Elford W.G., et al., 1998, Space Science Reviews, 84, 327

[4] Ceplecha Z., Borovicka J., Elford W.G., et al., 1998, Space Science Reviews, 84, 327

[5] Chang J.L., Avery S.K., Vincent R.A., 1999, Radio Sci., 34, 179

[6] Chapin E., Kudeki E., 1994, Geophys. Res. Lett., 21, 2433

[7] Chen F.F., 1984, Introduction to Plasma Physics and Controlled Fusion, 2nd ed, Plenum, New York

[8] Close S., Oppenheim M.M., Hunt S., Dyrud L.P., 2002, Journal of Geophysical Research, 107, in

[9] Dyrud L.P., Oppenheim M.M., vom Endt A.F., 2001, Geophysics Research Letters, 28, 2775

[10] Fejer B.G., Farley D.T., Balsley B.B., Woodman R.F., 1975, J. Geophys. Res., 80, 1313

[11] Fejer B.G., Providakes J., Farley D.T., 1984, J. Geophys. Res., 89, 7487

[12] Jones J., Jones W., 1991, Planet. Space Sci., 39, 1289

[13] Jones W., 1991, Planet. Space Sci., 39, 1283

[14] Kudeki E., Farley D.T., 1989, J. Geophys. Res., 94, 426

[15] Lee K., Kennel C.F., Kindel J.M., 1971, Radio sci., 6, 209

[16] Öpik E.J., 1958, Physics of Meteor Flight in the Atmosphere, Interscience Publishers

[17] Oppenheim M.M., vom Endt A.F., Dyrud L.P., 2000, Geophysics Research Letters, 27, 3173

[18] Pickering W.M., Windle D.W., 1970, Planet. Space Sci., 18, 1153

[19] Rishbeth H., Garriott O.D., 1969, Introduction to Ionospheric Physics, Academic

[20] Schmidt M.J., Gary S.P., 1973, J. Geophys. Res., 78, 8261

[21] Zhou Q.H., Mathews J.D., Nakamura T., 2001, Geophys. Res. Lett., 28, 1299